

# Contour lines of the discrete scale invariant rough surfaces

M. Ghasemi Nezhadhighi<sup>1</sup> and M. A. Rajabpour<sup>\*2</sup>

<sup>1</sup>*Department of Physics, Sharif University of Technology, Tehran, P.O.Box: 11365-9161, Iran*

<sup>2</sup>*SISSA and INFN, Sezione di Trieste, via Bonomea 265, 34136 Trieste, Italy*

We study the fractal properties of the  $2d$  discrete scale invariant (DSI) rough surfaces. The contour lines of these rough surfaces show clear DSI. In the appropriate limit the DSI surfaces converge to the scale invariant rough surfaces. The fractal properties of the  $2d$  DSI rough surfaces apart from possessing the discrete scale invariance property follow the properties of the contour lines of the corresponding scale invariant rough surfaces. We check this hypothesis by calculating numerous fractal exponents of the contour lines by using numerical calculations. Apart from calculating the known scaling exponents some other new fractal exponents are also calculated.

## I. INTRODUCTION

Discrete scale invariance (DSI) is a ubiquitous phenomenon in human made fractals and also in the fractals of nature. The list of applications of discrete scale invariance covers phenomena in a wide range of topics such as diffusion in anisotropic quenched random lattices [1], growth processes and rupture [2], non-extensive statistical physics [3], econophysics [4, 5], sociophysics [6], as well as quenched disordered systems [7] and cosmic lacunarity [8], for review of the concept and other applications see [9–11]. The signature of the presence of DSI is complex exponent which manifest itself in log-periodic corrections to scaling. In some cases the log-periodic oscillations appear in the time dependence of some physical quantities such as the energy release on the approach of impending rupture [12] and earthquakes [13] and in some other cases the DSI appears in the geometry of the system, the most famous cases being animals [7], diffusion limited aggregation (DLA) [14] and sandpile model on Sierpinski gasket [15]. Recently we found an other example in surface science, some of the rough surfaces as well as their contour lines show clear DSI in their geometry [16]. The rough surfaces have been the subject of intense studies for many years [17]. The first predictions of the scaling exponents of the contour lines of the scale invariant rough surfaces appeared in [18]. The scaling exponents predicted in [18] were confirmed numerically in [19] and the different applications of the findings in glassy interfaces and turbulence were discussed in [20]. After the invention of the stochastic Schramm-Loewner evolution [21] which describes scale invariant curves in two dimensions a revival appeared in the field and many new properties of the contour lines were investigated, for example see [22–24]. One of the most important findings of the paper [18] is the dependence of the different exponents of the contour lines to the only universal parameter in the system, i.e. roughness (*Hurst*) exponent. They showed that for the full scale invariant rough surfaces the fractal dimension of all of the contours  $d$ , the

fractal dimension of one contour  $D_f$  and the length distribution exponent  $\tau$  of the contour lines are just simple functions of the roughness exponent. Although there is no theoretical proof for the scaling relations found in [18] they were confirmed in many different numerical studies [19, 23].

The building block of the functions with DSI is Weierstrass-Mandelbrot (WM) function which was studied by Berry and Lewis in [25]. It is a random continuous non differentiable mono fractal function that one can see it in a wide range of physical phenomena such as sediment, turbulence [9, 10] and propagation and localization of waves in fractal media [26]. The function is scale invariant just for particular value of the scale parameter  $\gamma$ . It was shown in [16, 25] that in the  $\gamma \rightarrow 1$  limit the WM function converges to the Brownian motion. In the other words one can think about WM function as the perturbed Brownian motion which the perturbing parameter is the  $\gamma$ . The same argument is also true for the  $2d$  WM function [27, 28] and one can think about the  $2d$  WM function as the mono fractal rough surface with the DSI property for the specific value of  $\gamma$ . It was shown in [16] that up to the fractal dimension calculations many properties of the WM function is the same as the Brownian motion counterpart. What we are going to do in this paper is confirming this idea for the contour lines of the  $2d$  WM function. We will show numerically that many exponents of the contour lines of the  $2d$  WM function are the same as the exponents of the contour lines of the corresponding  $2d$  Brownian sheet. In other words we confirm the same scaling relations as the paper [18] for our discrete mono scale invariant contour lines.

The structure of the paper is as follows: In the next section we will introduce  $1d$  and  $2d$  Weierstrass-Mandelbrot function and we will discuss the DSI property of the surfaces. The third section is basically for fixing the notation and introducing different exponents, most of the materials of this section were already discussed in [18, 19]. In the forth section we will numerically confirm all the proposed scaling exponents and relations of the third section and we will show the universality of those relations. In the last section we will summarize our findings and we will give some comments about the possible future directions.

---

\*e-mail: rajabpour@sissa.it

## II. DEFINITION OF 1D AND 2D WEIERSTRASS-MANDELBROT FUNCTION

The Weierstrass-Mandelbrot (WM) function is a continuous non differentiable function. This function has discrete scale invariance property which is a weaker kind of scale invariance. In other words for the measurable quantity  $\mathcal{O}$ ; the relation  $\mathcal{O}(\lambda x) = \mu(\lambda)\mathcal{O}(x)$  occurs only for a special value of  $\lambda$ . The definition of the one dimensional WM function is

$$W(t) = \sum_{n=-\infty}^{\infty} \frac{g(\gamma^n t) e^{i\phi_n}}{\gamma^{(2-D)n}}; \quad (1)$$

where  $g(x)$  is a generic periodic function,  $\gamma > 1$ ,  $1 < D < 2$  and  $\phi_n$  is an arbitrary phase [25]. This function does not change under scaling transformation  $t \rightarrow bt$  if and only if  $b = \gamma$ . In this case WM function has self-affine scaling law

$$W(\gamma t) = \gamma^{2-D} W(t) = \gamma^H W(t), \quad (2)$$

where the parameter  $H = 2 - D$  is the *Hurst* exponent. The self affine scaling property of the WM function can be also seen in the correlation function of the increment  $\chi = \Delta W(t, \tau) = W(t + \tau) - W(t)$  of the process which is

$$C(\tau) = \langle |\chi|^2 \rangle_\phi = \sum_{n=-\infty}^{\infty} \frac{|g(\gamma^n(t + \tau)) - g(\gamma^n t)|^2}{\gamma^{2(2-D)n}}, \quad (3)$$

where phase  $\phi_n$  picked up from the uniform random distributed numbers. Since the condition  $C(\gamma\tau) = \gamma^{2(2-D)}C(\tau)$  is true for all periodic functions  $g(x)$ , therefore the correlation function is also scale invariant.

The Weierstrass-Mandelbrot function was generalized to two dimensions in [27] as follows

$$W(x, y) = C \sum_{\substack{m \in [1, M] \\ n \in (-\infty, \infty)}} A_m B_n G(r\eta_{m,n}) e^{i\phi_{m,n}}; \quad (4)$$

where  $C = (\ln\gamma/M)^{1/2}$ ,  $B_n = (k_0\gamma^n)^{D-3}$ ,  $\eta_{m,n} = k_0 \cos(\theta - \alpha_m)\gamma^n$ ,  $r = (x^2 + y^2)^{1/2}$  and  $\theta = \tan^{-1}(y/x)$ . The normalization factor  $C$  is chosen so that the correlation function  $V(\rho)$  be finite in the limits  $M \rightarrow \infty$  and  $\gamma \rightarrow 1$ . The  $A_m$  factor can control the isotropy of WM surface. We have an isotropic rough surface when  $A_m = A$ . The wave number  $k_0 = \frac{2\pi}{L}$  corresponds to system size  $L$  and for each  $m$  indices there is one phase  $\alpha_m$  that may be deterministic or stochastic. In this study  $\alpha_m = \frac{\pi m}{M}$  and  $\phi_{m,n}$  is selected randomly from the interval  $[0, 2\pi]$  with uniform distribution.

In numerical methods the two parameters  $M$  and  $n$  should be finite but large enough that  $W(x, y)$  does not change with increasing these parameters. Fractal dimension  $D$  and *Hurst* exponent  $H = 3 - D$  are two important

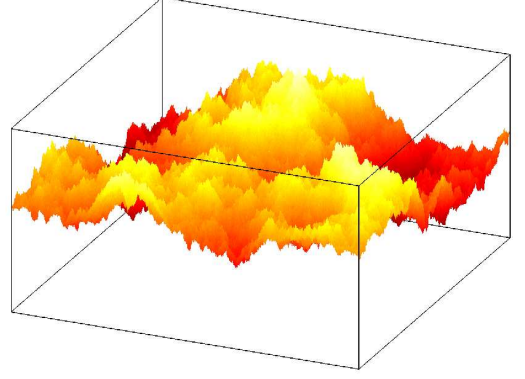


FIG. 1: (Color online) WM rough surfaces with  $H = 0.4$  and  $\gamma = 1.5$ . Light yellow (light Gray) regions correspond to larger heights and dark red (dark Gray) regions correspond to smaller heights.

parameters in simulating WM function, for an example of 2d WM function see Fig. 1. The surfaces with larger  $H$  seems smoother than the surfaces with smaller  $H$ .

The correlation function of the two dimensional WM function  $C(\rho) = \langle |W(\mathbf{r} + \rho) - W(\mathbf{r})|^2 \rangle_\phi$  obeys the scaling law  $C(\gamma\rho) = \gamma^{2(3-D)}C(\rho)$  where  $D$  is the fractal dimension and  $2 < D < 3$ . This shows that  $C(\rho)$  is also a self similar function.

One of the capabilities of WM function is that some of the statistical properties of this function do not have any sensitivity to the form of  $G(x)$ . We use  $1 - e^{ix}$  and  $\sin^{-1}(\sin(x))$  as  $G(x)$  in Eq. (4) and we will show that the statistical properties of the contour lines of 2d WM function depend only to the *Hurst* exponent of this process.

## III. SCALING LAWS OF THE CONTOUR LINES

For a given stochastic scale invariant rough surface with the height  $h(\mathbf{x})$ , a level set  $h(\mathbf{x}) = h_0$  for different values of  $h_0$  consists of many closed non-intersecting loops. These loops are scale invariant and their size distribution is characterized by a few scaling functions and scaling exponents. For example the contour line properties can be described by the loop correlation function  $G_l(\mathbf{r})$ . The loop correlation function measures the probability that two points separated with distance  $\mathbf{r}$  in the plane lie on the same contour. Rotational invariance of the contour lines forces  $G_l(r)$  to depend only on  $|\mathbf{r}|$ . This function for the contours on the lattice with grid size  $a$  and in the limit  $r \gg a$  has the scaling behavior

$$G_l(r) \sim \frac{1}{r^{2x_l}}, \quad (5)$$

where  $x_l$  is the loop correlation exponent.

Another measure associated with a given contour loop ensemble is  $G_s(r)$ . This probability is called the two point correlation function for contour lines with length  $s$ . Scaling properties of the contours force  $G_s(r)$  to scale with  $s$  and  $r$  as

$$G_s(r) \sim s^m |r|^{-n} f_{G_s}(r/R), \quad (6)$$

where  $m$  and  $n$  are two unknown exponents and  $f_{G_s}(r/R)$  is a scaling function. In this function we must scale  $r$  by the typical diameter  $R$  which is called radius of gyration. For one loop with  $N$  discrete points  $\{(x_1, y_1), \dots, (x_N, y_N)\}$ , the radius of gyration  $R$  is defined by

$$R^2 = \frac{1}{N} \sum_{i=1}^N \left( (x_i - x_c)^2 + (y_i - y_c)^2 \right), \quad (7)$$

where  $x_c = \frac{1}{N} \sum_{i=1}^N x_i$  and  $y_c = \frac{1}{N} \sum_{i=1}^N y_i$  are the central mass coordinates.

The 2d WM function is a self affine surface. A key consequence of this result is that, the contour lines with perimeter  $s$  and radius  $R$  of such surfaces are self-similar. When these lines are scale invariant one can determine the fractal dimension as the exponent in the perimeter-radius relation. The relation between contour length  $s$  and its radius  $R$  is

$$s \sim R^{D_f}, \quad (8)$$

where  $D_f$  is the fractal dimension,  $R$  is defined by Eq. (7) and  $s$  is measured with a ruler of length  $a$ . It is a right time to mention that the  $D_f$  is the fractal dimension of one contour and it is different from the fractal dimension of all the level set  $d$ . The latter one can be derived from the fractal dimension of the rough surface which is  $3 - H$  and the intersection rule of the Mandelbrot. Since the level set, the set of the contour lines, is the intersection of the rough surface with a two dimensional surface one can derive the following relation

$$d = 2 - H. \quad (9)$$

For a given self similar loop ensemble one can define the probability distribution of contour lengths  $\tilde{P}(s)$ . This function is a measure for the loops with length  $s$  and follows the power law

$$\tilde{P}(s) \sim s^{-\tau}, \quad (10)$$

where  $\tau$  is a scaling exponent. The above power law functions (Eqs. (6), (8) and (10)), introduce the geometrical exponents  $x_l$ ,  $D_f$  and  $\tau$ . These exponents depend only on the roughness exponent  $H$  [18].

One can derive mean loop length  $\langle s \rangle$  and the probability distribution of length  $\tilde{P}(s)$  from another quantity  $\tilde{n}(R, s)$ . This function is the probability distribution of contours with length  $(s, s + ds)$  and radius  $(R, R + dR)$ .

Scale invariance of the contours forces  $\tilde{n}(R, s)$  to scale with  $s$  and  $R$  as

$$\tilde{n}(R, s) \sim s^{-y} f_n(s/R^{D_f}). \quad (11)$$

In the above relation  $y$  is related to the fractal dimension  $D_f$  and the length distribution exponent  $\tau$ . It is obvious that

$$\langle s \rangle(R) = \frac{\int_0^\infty ds \tilde{n}(R, s) s}{\int_0^\infty ds \tilde{n}(R, s)}, \quad (12)$$

$$\tilde{P}(s) = \int_0^\infty dR \tilde{n}(R, s). \quad (13)$$

The above equations and Eq. (11) yield  $\tilde{P}(s) \sim s^{-y+1/D_f}$ , which we can equate this with Eq. (10), and obtain  $y = \tau + 1/D_f$ . Notice that, one can derive scaling law (8) from Eqs. (11) and (12).

Following [18] one can determine the relation between all geometrical exponents. In order to find the first scaling relation, one can use from the scale invariance of the rough surfaces, i.e.  $h(b\mathbf{x}) = b^H h(\mathbf{x})$  under  $\mathbf{x} \rightarrow b\mathbf{x}$ , and invariance of  $\tilde{n}(R)$  under rescaling, i.e.  $\tilde{n}(R/b) = b^{3-H} \tilde{n}(R)$ , then

$$\tilde{n}(R) \sim R^{-3+H}. \quad (14)$$

On the other hand, the number of loops with radius in  $(R, R + dR)$  can be derived from  $\tilde{n}(R) = \int_0^\infty ds \tilde{n}(R, s)$ , where it obeys the scaling law

$$\tilde{n}(R) \sim R^{-(1+D_f(\tau-1))}. \quad (15)$$

Equations (14) and (15) lead to the first scaling relation

$$D_f(\tau - 1) = 2 - H. \quad (16)$$

This relation is called hyperscaling relation; it is derived for the scale invariant rough surfaces. The above argument is also true for the discrete scale invariant surfaces such as 2d WM functions. For the DSI rough surfaces such as Eq. (4), condition  $h(b\mathbf{x}) = b^H h(\mathbf{x})$  is true just for a special value of  $b = \gamma$ .

For a self affine random field, there is another scaling relation that connect the three geometrical exponents  $D_f$ ,  $\tau$  and  $x_l$ . This relation is derived from a sum rule [18]. Integrating (6) over all lattice points gives the total number of points on the loop

$$s = \int d^2\mathbf{r} G_s(\mathbf{r}) \sim s^{(2-n)/D_f+m}. \quad (17)$$

The above equality gives one relation between the exponents  $n$  and  $m$  as

$$2 - n = D_f(1 - m). \quad (18)$$

The integration of  $G_s(\mathbf{r})$  over loop probability distribution function  $P(s) = s\tilde{P}(s)$  gives the total loop correlation function  $G_l(r)$

$$G_l(r) = \int ds P(s) G_s(\mathbf{r}) \sim r^{-n} (r^{D_f})^{m+2-\tau}, \quad (19)$$

where after using Eqs. (5) and (19) gives another relation between  $m$  and  $n$  as

$$-n + D_f(m + 2 - \tau) = -2x_l. \quad (20)$$

Elimination of  $m$  and  $n$  from equations (18) and (20) leads to the second scaling relation

$$D_f(3 - \tau) = 2 - 2x_l. \quad (21)$$

If we combine the two scaling relations (16) and (21) we can find two exponents  $D_f$  and  $\tau$  as a function of the *Hurst* exponent  $H$  and the loop correlation exponent  $x_l$ ,

$$D_f = 2 - x_l - \frac{H}{2}, \quad (22)$$

and

$$\tau = 1 + \frac{2 - H}{2 - x_l - H/2}. \quad (23)$$

In the next section we will numerically calculate all the introduced exponents related to the contour lines of DSI rough surfaces and we will show that the two scaling relations (16) and (21) are valid for generic 2d-WM function.

#### IV. NUMERICAL RESULTS

To simulate the 2d WM function on the discrete lattice we used lattices on square grid with sizes 1024 and 2048. In equation (4) we set  $M = 20$  and  $-n_{min} = n_{max} = 50$ . After setting  $\gamma = 1.5$  we simulated the WM rough surfaces with the *Hurst* parameter in the range of  $H = \{0.0, 0.1, 0.2, 0.3, 0.4, 0.5, 0.6\}$  for two periodic functions  $G(x) = (1 - e^{ix})$  and  $G(x) = \sin^{-1}(\sin(x))$ . In each case, all numerical tests have been done using from 250 realizations. The contouring algorithm followed from [23] to generate contour lines of rough surfaces. In Fig. 2 one can see that the number of loops increases by decreasing roughness exponent.

We would like to measure the exponents  $d$ ,  $D_f$ ,  $\tau$  and  $x_l$  with a large enough loop ensemble for the mentioned values of the *Hurst* exponents. Before starting numerical computation of the geometrical exponents, it is important to see the DSI property in the contour lines of such discrete scale invariant rough surfaces. At the beginning we will show that the contour lines of DSI rough surfaces are discrete scale invariant. Existence of DSI in the loop ensemble can be studied by the Lomb normalized periodogram test.

##### A. The Lomb normalized periodogram

The 2d Weierstrass Mandelbrot function (4) is a discrete scale invariant function which can be constructed

by using periodic function  $G(x)$  with infinite number of discrete frequencies  $\omega_n = \gamma^n$ . Each frequency contributes in (4) with weight  $\gamma^{-Hn}$ . To detect these frequencies one can use the Lomb normalized periodogram.

For a given time series  $X_i \equiv X(t_i)$  with  $N$  data points, this kind of spectral analysis fitting these data points to a sine function of varying frequencies by least square method [29]. Lomb analysis measures spectral power  $P(\omega)$  as a function of angular frequency  $\omega$  as

$$P_N(\omega) = \frac{1}{2\sigma^2} \left( \frac{[\sum_j (X_j - \bar{X}) \cos \omega(t_j - \delta)]^2}{\sum_j \cos^2 \omega(t_j - \delta)} + \frac{[\sum_j (X_j - \bar{X}) \sin \omega(t_j - \delta)]^2}{\sum_j \sin^2 \omega(t_j - \delta)} \right); \quad (24)$$

where  $\bar{X} = \frac{1}{N} \sum_1^N X_i$ ,  $\sigma^2 = \frac{1}{N-1} \sum_1^N (X_i - \bar{X})^2$  and  $\delta$  is defined by the relation  $\tan(2\omega\delta) = \frac{\sum_j \sin 2\omega t_j}{\sum_j \cos 2\omega t_j}$ .

We used from Lomb test to show that the contour lines of the DSI rough surfaces are discrete scale invariant. For a closed loop (see Fig. 3), with  $N$  data points  $\{(x_1, y_1), \dots, (x_N, y_N)\}$ , the distance from the center of mass; i.e.  $r(i) = \left( (x_i - x_c)^2 + (y_i - y_c)^2 \right)^{1/2}$ , where  $x_c = \frac{1}{N} \sum_{i=1}^N x_i$  and  $y_c = \frac{1}{N} \sum_{i=1}^N y_i$  are the center of mass coordinates; is a good quantity to detect the discrete frequencies. Using Lomb test we measured  $\gamma_{exp} = \langle \omega_{i+1} / \omega_i \rangle = 1.55 \pm 0.04$  where  $\omega_{i+1}$  and  $\omega_i$  are two frequencies that  $P(\omega)$  has sharp picks, results are shown in Fig. 4. This result is in a good agreement with the theoretical value of  $\gamma = 1.5$ .

##### B. Loop correlation exponents

In this subsection we will numerically find the most fundamental exponents of the contour lines of the rough surfaces, i.e.  $x_l$  and  $n$ , by analyzing the functions  $G_s(r)$  and  $G_l(r)$ .

###### 1. Scaling exponents in $G_l(r)$

To find the correlation function from a given loop ensemble we follow the algorithm described in [18]. Using scaling properties of loop correlation function we can measure correlation exponent  $x_l$ . For the large class of rough surfaces  $x_l = \frac{1}{2}$ , this scaling exponent is independent of  $H$  [18]. Our numerical tests show that  $x_l = 0.5 \pm 0.05$  for all the WM rough surfaces and it is not a function of  $H$  or  $G(x)$  as shown in Fig. 5.

###### 2. Scaling exponents in $G_s(r)$

The scaling behavior of the two point correlation function of the contours with length  $s$  is defined in Eq. (6).

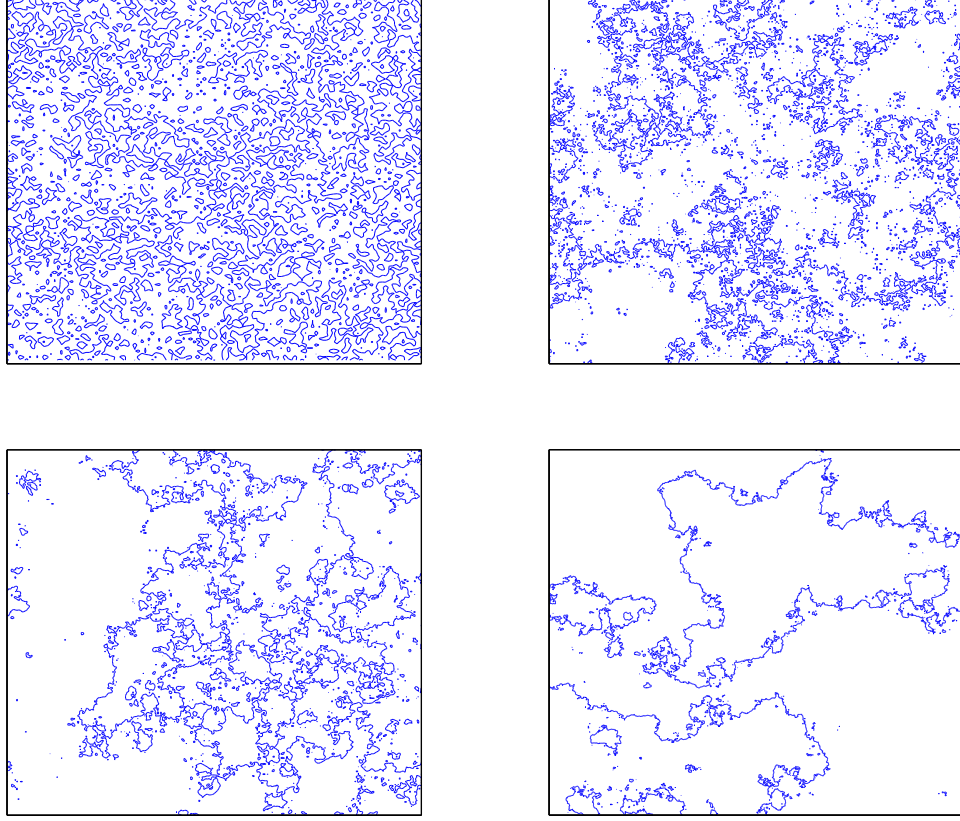


FIG. 2: (Color online) Small parts of contour lines of 2d WM rough surface with  $G(x) = (1 - e^{ix})$  and lattice size  $1024^2$ . Top left ( $H = 0.0$ ), right ( $H = 0.2$ ), and bottom left ( $H = 0.4$ ), right ( $H = 0.6$ ).

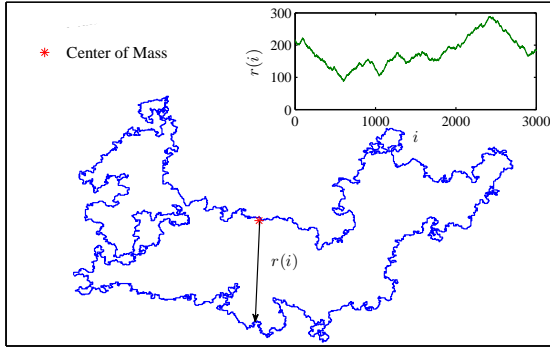


FIG. 3: (Color online) Largest contour line of 2d WM rough surfaces with  $N = 6 \times 10^3$ ,  $D = 2.5$  and  $\gamma = 1.5$ . Distance  $r(i)$  for each point  $i$  from the center of mass is shown in the inset.

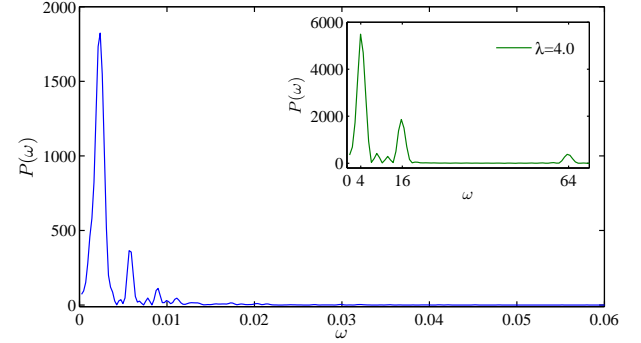


FIG. 4: (Color online) Lomb test on the contour line of 2D WM surfaces with  $D = 2.5$  and  $\gamma = 1.5$ . Lomb test on 1d WM time series with  $\gamma = 4.0$ , is shown in the inset. Sharp picks show that the contour lines of WM surfaces are DSI.

The exponent  $n$  can be measured from the power law dependence of  $G_s(r)$  with respect to  $r$  for a fixed value of the perimeter  $s$ , see Fig. 6. For this purpose the contour loops with the perimeter in the range  $(s, \alpha s)$  ( $\alpha > 1$ )

are considered and  $G_s(r)$  is measured as a function of  $r$  for the different values of  $s$ , see Table 1. There is neither theoretical prediction for this exponent and nor any numerical estimates. Our numerical calculation shows

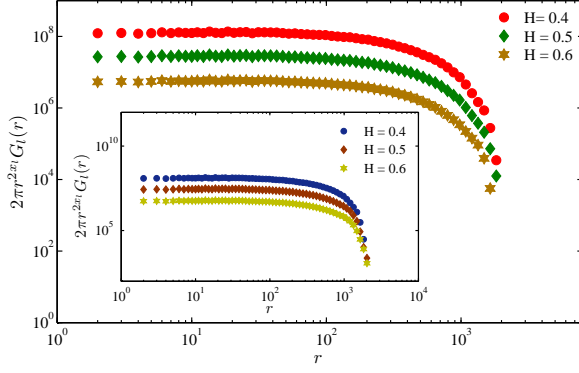


FIG. 5: (Color online) The loop correlation function for the DSI rough surfaces with  $H = 0.4, 0.5$  and  $0.6$  (from top to bottom) for  $G(x) = 1 - e^{ix}$ . The loop correlation function for  $G(x) = \sin^{-1}(\sin(x))$  is shown in the inset. The plots were derived for the system size  $L = 2048$  and  $\gamma = 1.5$ .

that the exponent  $n$  closely follows the relation  $\frac{1+H}{2}$ , see Fig. 7 which means that the exponent  $m$  is very small compared to the exponent  $n$ . Our numerical calculation shows that the same values can also be derived for the scaling mono fractal rough surfaces.

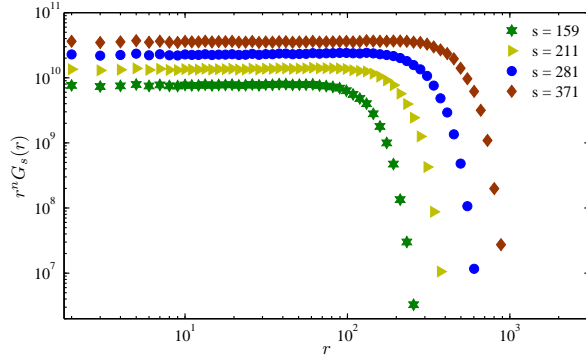


FIG. 6: (Color online) The scaling behaviour of  $G_s(r)$  as a function of  $r$  in the DSI rough surfaces for  $G(x) = 1 - e^{ix}$  with  $L = 2048$ ,  $H = 0.5$  and  $\gamma = 1.5$ .

### C. Fractal dimensions

To study the fractal properties of contour lines, the fractal dimension of loops  $D_f$  and the fractal dimension of all the contours  $d$ , in DSI rough surfaces one can use from three related approaches. In the first method one can use from self-similar properties of contours to measure fractal dimensions. The second method is using cumulative distribution of area and the last one is the Zipf's law. We used these three methods to find the two geometrical exponents  $D_f$  and  $d$ .

#### a. Length-radius scaling relation:

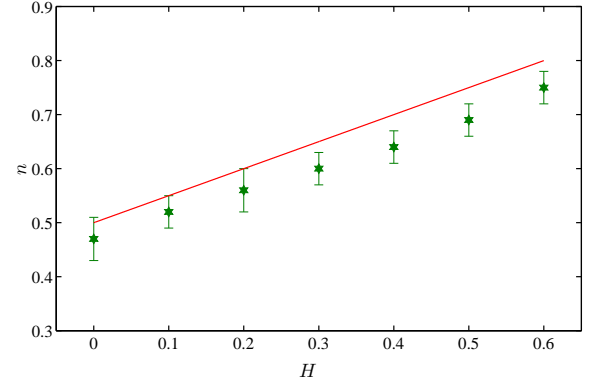


FIG. 7: (Color online) The exponent  $n$  with respect to the roughness exponent  $H$  for  $G(x) = 1 - e^{ix}$ . The slope of the best fit line is  $0.45 \pm 0.03$ . The smooth line is the line  $n = \frac{1+H}{2}$ .

$H$	$G(x) = 1 - e^{ix}$	$G(x) = \sin^{-1}(\sin(x))$
0.0	$0.46 \pm 0.04$	$0.47 \pm 0.03$
0.1	$0.53 \pm 0.03$	$0.52 \pm 0.03$
0.2	$0.56 \pm 0.04$	$0.56 \pm 0.02$
0.3	$0.59 \pm 0.03$	$0.59 \pm 0.04$
0.4	$0.64 \pm 0.03$	$0.64 \pm 0.03$
0.5	$0.69 \pm 0.03$	$0.69 \pm 0.04$
0.6	$0.74 \pm 0.03$	$0.75 \pm 0.03$

TABLE I: The numerical values of the scaling exponent  $n$  derived from the two point correlation function  $G_s(r)$ .

In order to find the fractal dimension of the contours  $D_f$  we used directly from the scaling relation between loop perimeter  $s$  and the radius of gyration  $R$  according to Eq. (8). Scaling behavior of the averaged loop length  $\langle s \rangle$  with respect to  $R$  in log-log plot is shown in Fig. 8. The geometrical exponent  $D_f$  is measured using the least-square linear fit in the scaling regime ( $10 < R < 100$ ).

The fractal dimension of all contours  $d$  can be found by box counting method [31]. This method is based on the self similar properties of all contours in the level set. For a self similar object there is a scaling law between the number of boxes  $N(L)$  with size  $L$  needed to cover the fractal object

$$N(L) \sim L^{-d}. \quad (25)$$

As shown in Fig. 9, we find excellent agreement between a measured values of  $D_f$  and  $d$  with theoretical predictions.

#### b. Cumulative distribution of areas:

The cumulative distribution of the loop area is a good measure to describe the fractal dimension of the set of all contour lines  $d$  [23]. For a self affine random field the number of contours with area greater than  $A$  has the

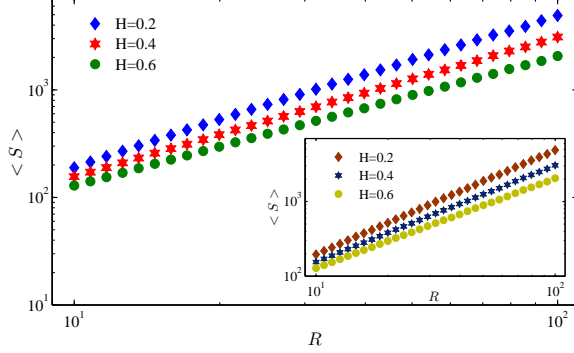


FIG. 8: (Color online) The scaling relation between the averaged loop length  $\langle s \rangle$  and the radius of gyration  $R$  for contour lines of the DSI rough surfaces with  $G(x) = 1 - e^{ix}$ . The same scaling behavior for  $G(x) = \sin^{-1}(\sin(x))$  is shown in the inset.

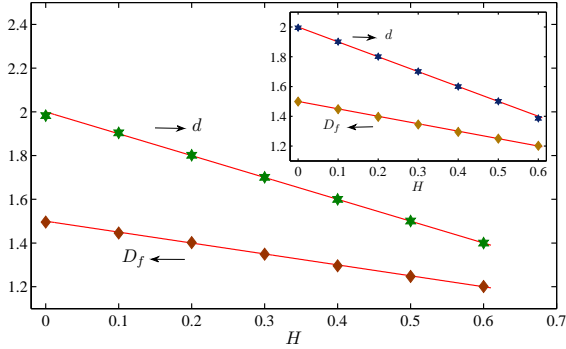


FIG. 9: (Color online) The fractal dimension of all contours  $d$  and the geometrical exponent  $D_f$  as a function of  $H$  for the DSI surfaces with  $G(x) = 1 - e^{ix}$ . These scaling exponents for  $G(x) = \sin^{-1}(\sin(x))$  are shown in the inset. The solid lines correspond to the theoretical predictions.

scaling form

$$N_{>}(A) \sim A^{-d/2}, \quad (26)$$

where  $d = 2 - H$ . An example of the scaling behaviour in cumulative distribution of area is shown in Fig. 10. Here, we plot  $N_{>}(A)$  as a function of  $A$  for  $H = 0.4$  in log-log plot, to show how they follow Eq. (26). In Table II we report the scaling exponent  $d/2$  for different values of  $H$ .

### c. Zipf's laws

Zipf's law is one of the most prominent examples of power laws in nature [23, 30–33]. If we assign ranks to a measurable quantity  $\mathcal{M}_n$  according to their size, there is an interesting power law relation in the size-rank distribution which is called by Mandelbrot the Zipf's law. In this method the greatest one measured quantity has rank 1 ( $\mathcal{M}_1$ ), smaller rank 2 ( $\mathcal{M}_2$ ) and so on. Zipf's law states that the ranked size  $\mathcal{M}_n$  falls off as

$$\mathcal{M}_n \sim n^{-\gamma}, \quad (27)$$

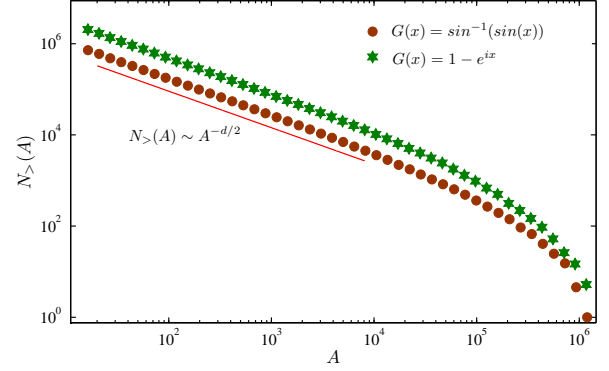


FIG. 10: (Color online) Cumulative number of loops whose area is greater than  $A$  for the DSI rough surfaces with  $G(x) = 1 - e^{ix}$  and  $G(x) = \sin^{-1}(\sin(x))$  with  $H = 0.4$ , system size  $L = 2048$  and  $\gamma = 1.5$ .

$H$	Theory	$G(x) = 1 - e^{ix}$	$G(x) = \sin^{-1}(\sin(x))$
0.0	1.00	$1.00 \pm 0.01$	$1.00 \pm 0.01$
0.1	0.95	$0.96 \pm 0.01$	$0.96 \pm 0.01$
0.2	0.90	$0.91 \pm 0.01$	$0.90 \pm 0.01$
0.3	0.85	$0.86 \pm 0.01$	$0.86 \pm 0.01$
0.4	0.80	$0.81 \pm 0.01$	$0.81 \pm 0.01$
0.5	0.75	$0.76 \pm 0.01$	$0.77 \pm 0.02$
0.6	0.70	$0.71 \pm 0.01$	$0.71 \pm 0.01$

TABLE II: The best fit values of the exponent  $d/2$  derived from the scaling laws of cumulative distribution  $N_{>}(A)$ .

where  $\gamma$  is a scaling exponent. The scaling laws (27) for  $\mathcal{M}_n = \{l_n, A_n, R_n\}$  with  $l_n$ ,  $A_n$  and  $R_n$  are in order, the ranked perimeter, ranked area and ranked radius of gyration, are

$$l_n \sim n^{-D_f/d}, \quad A_n \sim n^{-2/d}, \quad R_n \sim n^{-1/d}, \quad (28)$$

where  $D_f$  is the fractal dimension of contours and  $d$  is the fractal dimension of all loops. We calculated the exponents in Eq. (28) for 2D WM rough surfaces using numerical tests. Averaged values over different realizations for each exponents in Eq. (28) as a function of  $H$  is presented in Figs. 11.

### D. Length distribution exponent

The loop exponent  $\tau$  can be extracted from  $\tilde{P}(s)$  which follows Eq. (10). This probability distribution function at large  $s$  has the statistical noise. In order to minimize these noises, we consider the cumulative distribution of loop length  $\tilde{P}_{>}(s) = \int_s^\infty \tilde{P}(s') ds'$  with the scaling form  $\tilde{P}_{>}(s) \sim s^{-\tau+1}$ . The length distribution exponent  $\tau$  can be measured numerically from the power-law scaling in loop length ( $10 < s < 1000$ ). The scaling behavior of



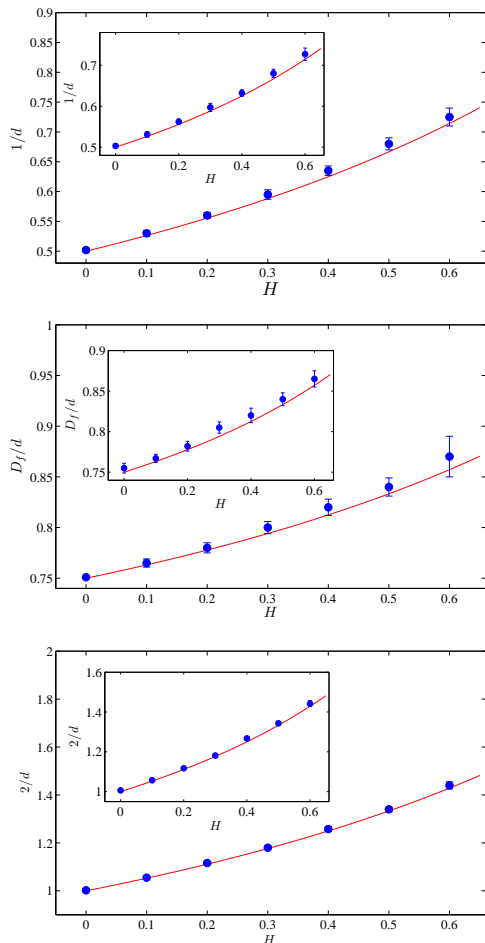


FIG. 11: (Color online) The numerical estimation for the scaling exponents: top  $1/d$ , middle  $D_f/d$  and bottom  $2/d$ ; for the WM rough surfaces with  $G(x) = 1 - e^{ix}$  and the system size  $L = 2048$ . The numerical computation of each exponents for the rough surfaces with  $G(x) = \sin^{-1}(\sin(x))$  are shown in the insets. The solid lines show the theoretical relation between  $1/d$ ,  $D_f/d$  and  $2/d$  with the Hurst exponent  $H$ .

the cumulative distribution  $\tilde{P}_>(s)$  for  $H = 0.5$  is plotted in Fig. 12 for different periodic functions  $G(x)$ . The deviation from scaling line at large  $s$  comes from finite size effects. Numerical results for the exponent  $1 - \tau$  are summarized in Table III.

## V. CONCLUSION

In this paper we first introduced a wide range of rough surfaces with the discrete scale invariance property (4). The surfaces in the limit  $\gamma \rightarrow 1$  converge to the Gaussian mono fractal rough surfaces. The contour lines of the introduced curves show clear DSI property. The fractal dimension of the contours follow the behavior of the fixed point, i.e. Brownian sheet. The numerical calcu-

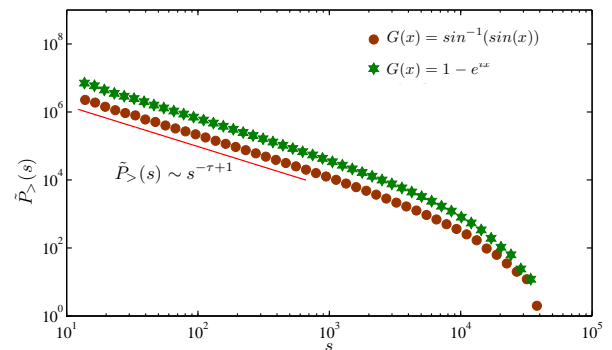


FIG. 12: (Color online) Cumulative loop-size distribution, for DSI rough surfaces with  $H = 0.5$  and system size  $L = 2048$ . Note that this plot shows that the scaling exponent  $\tau$  is independent of  $G(x)$ .

$H$	Theory	$G(x) = 1 - e^{ix}$	$G(x) = \sin^{-1}(\sin(x))$
0.0	-1.33	$-1.33 \pm 0.01$	$-1.34 \pm 0.01$
0.1	-1.31	$-1.31 \pm 0.01$	$-1.32 \pm 0.01$
0.2	-1.29	$-1.29 \pm 0.01$	$-1.29 \pm 0.01$
0.3	-1.26	$-1.27 \pm 0.01$	$-1.26 \pm 0.01$
0.4	-1.23	$-1.24 \pm 0.01$	$-1.24 \pm 0.01$
0.5	-1.20	$-1.21 \pm 0.01$	$-1.21 \pm 0.01$
0.6	-1.17	$-1.18 \pm 0.01$	$-1.18 \pm 0.01$

TABLE III: The best fit values of the exponent  $1 - \tau$  derived from the scaling laws of cumulative distribution  $\tilde{P}_>(s)$ .

lation shows that the relation  $x_l = \frac{1}{2}$  is superuniversal which means that it is independent of  $G(x)$ ,  $H$  and  $\gamma$ . Instead the exponent  $n$  changes linearly with respect to the roughness exponent  $H$ . We also checked numerically the consistency scaling exponent relations, i.e. (16) and (21). There are different methods to define WM rough surfaces in two dimensions, for a different example see [28], we strongly believe that the same scaling relations also hold for these surfaces. Although the relations that we introduced in section 3 are valid for almost all the mono fractal surfaces the careful studies of the multi fractal surfaces shows huge discrepancies [34].

Our calculation shows that it is possible to study the DSI version of the contour lines of the scale invariant rough surfaces. The DSI property does not change the fractal dimension of the curves. It seems that this is a very general property [16] and possibly can be seen in a wide range of statistical models. In other words it should be possible to change the usual statistical models in a particular way to have DSI property with the similar fractal properties as the ordinary statistical mechanics models.

Up to know the only difference of our models with the scale invariant rough surfaces is the DSI property. It is quite natural to try to find some other quantities that can



distinguish the continuous scale invariant rough surfaces from the discrete scale invariant rough surfaces. Since most of the well-known statistical models at the critical point show universality and in some cases conformal invariance it seems that we need a better understanding of discrete scale invariant field theories.

## ACKNOWLEDGMENTS

M. G. Nezhadhighi would like to thank S. Hosseinabadi for many helpful discussions, and also H. Hadipour and R. Mozaffari for computer supports.

- 
- [1] D. Stauffer, D. Sornette: *Physica A* 252 (1998) 271
  - [2] J. C. Anifrani, C. Le Floch, D. Sornette, B. Souillard: *J. Phys. I (France)* 5 (1995)631
  - [3] F. A. B. F. de Moura , U. Tirnakli, M. L. Lyra , *Phys. Rev. E* 62 (2000)6361-6365
  - [4] N. Vandewalle and M. Ausloos, *Eur. J. Phys. B* 4 (1998) 139 - 141; N. Vandewalle, M. Ausloos, Ph. Boveroux and A. Minguet, *Eur. J. Phys. B* 9 (1999) 355-359 and M. Ausloos and K. Ivanova, *New Directions in Statistical Physics - Econophysics, Bioinformatics, and Pattern Recognition*, L. T. Wille, Ed. (Springer Verlag, Berlin, 2004) p. 93-114
  - [5] S. Drozd, F. Ruf, J. Speth, M. Wojcik, *Eur. Phys. J. B* 10 (1999) 589-593; S. Drozd, M. Forczek, J. Kwapien, P. Oswiecimka and R. Rak, *Physica A* 383 (2007); 59-64 and P. Oswiecimka, S. Drozd, J. Kwapien, and A.Z. Gorski, *Acta Phys. Pol. A*, 117 (2010) 634-639
  - [6] W.-X. Zhou, D. Sornette, R. A. Hill, R. I.M. Dunbar, *PRSB* 272 (2005) 439-444
  - [7] H. Saleur and D. Sornette, *J. Phys. I France* 6 (1996) 327-355
  - [8] G. de Vaucouleurs, *Science* 167 (1970) 1203 and A. Provenzale, E.A. Spiegel and R. Thieberger, *CHAOS* 7 (1997) 82
  - [9] D. Sornette, *Physics Reports* 297 (1998) 239-270[cond-mat/9707012]
  - [10] D. Sornette, *Critical Phenomena in Natural Sciences. Chaos Fractals, Selforganization and Disorder: Concepts and Tools*(2000) Heidelberg, Germany: Springer-Verlag.
  - [11] B. Dubrulle, F. Garner, and D. Sornette (Eds.), *Scale invariance and beyond* (EDP Sciences and Springer, Berlin, 1997).
  - [12] J.-C. Anifrani, C. Le Floch, D. Sornette and B. Souillard, *J.Phys.I France* 5, n6 (1995) 631-638
  - [13] H. Saleur, C.G. Sammis and D. Sornette, *Nonlinear Processes in Geophysics* 3, No. 2 (1996)102-109; H. Saleur, C.G. Sammis and D. Sornette, *J.Geophys.Res.* 101 (1996) 17661-17677 and A. Johansen, D. Sornette, H. Wakita, U. Tsunogai, W. I. Newman, H. Saleur: *J. Phys. I (France)* 6 (1996)1391
  - [14] D. Sornette, A. Johansen, A. Arneodo, J.-F. Muzy and H. Saleur, *Phys. Rev. Lett.* 76 (1996) 251-254
  - [15] B. Kutnjak-Urbanc, S. Zapperi, S. Milojević, and H. Eugene Stanley, *Phys. Rev. E* 54 (1996) 272277 and M. Ausloos, K. Ivanova and N. Vandewalle, *Empirical sciences of financial fluctuations. The advent of econophysics*, Tokyo, Japan, Nov. 15-17, 2000 Proceedings H. Takayasu, Ed. (Springer Verlag, Berlin, 2002) pp. 62-76
  - [16] M. Ghasemi Nezhadhighi, M. A. Rajabpour, *Phys. Rev. E* 82 (2010)061101 [arXiv:1010.1631]
  - [17] A.-L. Barabasi and H. E. Stanley, *Fractal Concepts in Surface Growth* Cambridge University Press, New York, 1995.
  - [18] J. Kondev and C. L. Henley, *Phys. Rev. Lett.* 74 (1995) 4580
  - [19] J. Kondev, C. L. Henley, and D. G. Salinas, *Phys. Rev. E* 61 (2000) 164
  - [20] C. Zeng, J. Kondev, D. McNamara, and A. A. Middleton, *Phys. Rev. Lett.* 80 (1998)109 and J. Kondev, G. Huber, *Phys. Rev. Lett.* 86, (2001)26
  - [21] O. Schramm, *Israel J. Math.* 118 (2000)221- 288 [math/9904022]
  - [22] A. A. Saberi, M. A. Rajabpour, S. Rouhani, *Phys. Rev. Lett.* 100 (2008) 044504 [arXiv:0712.2984]
  - [23] M. A. Rajabpour and S. M. Vaez Allaei, *Phys. Rev. E* 80 (2009) 011115 [arXiv:0907.0881]
  - [24] A.A. Saberi, H. Dashti-Naserabadi, S. Rouhani, *Phys. Rev. E* 82, 020101(R) (2010) [arXiv:1007.4000]
  - [25] M.V. Berry, Z. V. Lewis, *Proc. R. Soc. Lond. A* 370 (1980) 459-484
  - [26] A. M. Garcia-Garcia, E. Cuevas [arXiv:1005.0266v]
  - [27] M. Ausloos and D.H. Berman, *Proc. R. Soc. London, Ser. A* 400 (1985) 331
  - [28] K. Falconer, *Fractal geometry: mathematical foundations and applications*, Wiley, Chichester, UK (2003).
  - [29] H. William *Numerical recipes: the art of scientific computing* 2nd Edition Press - 1992 Cambridge University Press
  - [30] B. B. Mandelbrot, *Fractals and scaling in finance* (springer, New York, 1997).
  - [31] B. B. Mandelbrot, *The fractal geometry of nature* (Freeman, New York, 1982).
  - [32] N. Jan, D. Stauffer, and A. Aharony, *J. Stat. Phys.* **92**, 325 (1998).
  - [33] B. Corominas-Murtra and D. Ricard V. Sol, *Phys. Rev. E* 82, (2010) 011102 [arXiv:1001.2733v2]
  - [34] S. Hosseinabadi, S. M. Vaez Allaei, M. S. Movahhed, M. A. Rajabpour, *in preparation*